

## Supplementary Information

# Indole-Substituted Flavonol-Based Cysteine Fluorescent Sensing and Subsequent Precisely Controlled Linear CO Liberation

### Table of Contents

#### Experimental Section

Materials and Instruments.

Preparation of Solutions.

Optical Responses

Kinetic Measurements

Optical Titrations of Probe by Cys

Cell Culture and Cytotoxicity Assay

Cell Fluorescence Imaging

Zebrafish Fluorescence Imaging

CO Photo-releasing Reaction Kinetics and Products Analysis

Synthesis of the Probe **MICA**.

#### Table Caption

**Table S1.** Comparison of the flavonol-based fluorescent probes.

#### Figure Caption

**Figure S1.** (a) Molecular orbital plots of HOMO and LUMO of the optimized structure of **MICA** and **HMIC** and their energy levels. (b) The theoretically predicted absorption spectra of **MICA** and **HMIC**.

**Figure S2.** Spectral features of **HMIC** (5  $\mu$ M) in various solvents.

**Figure S3.** (a) Fluorescence and (b) absorption spectra of **MICA**, **MICA** + 10 equiv. Cys and **HMIC**. Inset: The solution of **MICA**, **MICA** + 10 equiv. Cys, **HMIC** under 365 nm light.

**Figure S4.** Kinetic studies of the reaction of **MICA** with varying amounts of Cys at 37 °C. (a) Time traces of  $I_{464\text{ nm}}$  of **MICA** with Cys. (b) Plot of  $\ln[(I_t - I_\infty)/(I_0 - I_\infty)]$  of  $I_{464\text{ nm}}$  vs. time (for 10 equiv. Cys). (c) Time traces of  $A_{397\text{ nm}}$  of **MICA** with Cys.

**Figure S5.** (a) HPLC spectra of **MICA**, **HMIC**, reaction mixture of **MICA** with 10 equiv. Cys after 2 and 10 min. (b) TLC photos of **MICA**, **MICA** + 10 equiv. Cys, **HMIC**.

**Figure S6.** APCI–MS spectrum of the reaction solution of **MICA** with 10 equiv. Cys.

**Figure S7.** Fluorescence spectral changes of **MICA** upon addition of 10 equiv. Cys under (a) absence and (b) presence of 10 equiv. another competitive single amino acid. (c)  $I_{464\text{ nm}}$  of **MICA** upon addition of 10 equiv. Cys under absence (black) and presence (cyan) of 10 equiv. another competitive single amino acid.

**Figure S8.** Fluorescence spectral changes of **MICA** upon addition of 10 equiv. Cys under (a) absence and (b) presence of 10 equiv. another competitive single bio-relevant anion. (c)  $I_{464\text{ nm}}$  of **MICA** upon addition of 10 equiv. Cys under absence (black) and presence (cyan) of 10 equiv. another competitive single anion.

**Figure S9.** Fluorescence spectral changes of **MICA** upon addition of 10 equiv. Cys under (a) absence and (b) presence of 10 equiv. another single competitive single bio-relevant cation. (c)  $I_{464\text{ nm}}$  of **MICA** upon addition of 10 equiv. Cys under absence (black) and presence (cyan) of 10 equiv. another single competitive single cation.

**Figure S10.** The pH-dependent  $I_{464\text{ nm}}$  of **MICA** solution in the absence and presence of 10 equiv. Cys.

**Figure S11.** The MTT assay of HeLa cells respectively incubated with (a) **HMIC**, (b) **MICA** and (c) the **HMIC** photolysis products for 24 h.

**Figure S12.** The time traces of  $A_{379\text{ nm}}$  of **MICA** under the presence of the esterase.

**Figure S13.** (a) Fluorescence and (b) absorption spectral changes of **HMIC** during visible light irradiation under  $O_2$  at rt. Insets: Plots of (a)  $I_{464\text{ nm}}$  and (b)  $A_{397\text{ nm}}$  vs. the irradiation time.

**Figure S14.** HPLC-MS spectra for the photo-reaction organic products.

**Figure S15.** (a) Cyclic voltammograms of **HMIC** under  $N_2$ , subsequently under air. (b) Absorption spectral change of **HMIC** in the absence and presence of NBT under  $O_2$ .

**Figure S16.** FT-IR spectra of **MICA**.

**Figure S17.**  $^1H$  NMR spectrum of **MICA**.

**Figure S18.**  $^{13}C$  NMR spectrum of **MICA**.

**Figure S19.** HRMS spectrum of **MICA**.

**Figure S20.**  $^1H$  NMR spectrum of **HMIC**.

**Figure S21.**  $^{13}C$  NMR spectrum of **HMIC**.

## Experimental

### Materials and Instruments

The chemicals and reagents used in this experiment are of analytical grade or chromatographic grade and further purified by the standard method if necessary. FT-IR spectra were recorded with a Nicolet 6700 spectrophotometer.  $^1\text{H}$  NMR and  $^{13}\text{C}$  NMR spectra were recorded on a Bruker instrument at 400 MHz and 500 MHz, respectively (TMS as the internal standard). UV-vis spectra were measured using an Agilent Technologies HP8453 diode array spectrophotometer. The fluorescence spectra were recorded on an FL 6500 fluorescence spectrophotometer (Perkin Elmer Co., Ltd.). ESI-MS (electrospray ionization mass spectra) measurements were performed on Agilent Technologies HP1100LC-MSD. The organic reaction products analysis was performed on a Thermo Fisher Scientific LTQ Orbitrap XL HPLC-MS. The CO concentration was determined by using a GC (Techcomp 7900, Shanghai Jingke). The cytotoxicity assay was accomplished using the MTT method with a microplate reader (Infinite M200 Pro). The Cell images were performed with a confocal laser scanning microscope (LEICA TCS SP5 II, Germany). All bright-field and luminescence zebrafish images were performed on a fluorescence microscope (Nikon TE2000-E). Cyclic voltammetry data was collected using a CHI620b system. All CV data were obtained under  $\text{N}_2$  in DMF with an **HMIC** concentration of 2 mM and  $\text{Bu}_4\text{NBF}_4$  (0.1 M) as the supporting electrolyte. The scan rate was  $50 \text{ mV s}^{-1}$ . The experimental setup consisted of a glassy carbon working electrode, a silver reference electrode and a platinum wire auxiliary electrode. All potentials are reported vs. SCE.

### Preparation of Solutions.

The stock solutions of **MICA** (1.0 mM) and **HMIC** (1.0 mM) were prepared in DMF. The stock solutions (10 mM of each) of various amino acids (Cys, Homocysteine (Hcy), Glutathione (GSH, 20 mM), Lysine (Lys), Arginine (Arg), Alanine (Ala), Threonine (Thr), Methionine (Met), Asparagine (Asn), Isoleucine (Ile), Aspartic acid (Asp), Valine (Val), Serine (Ser), Proline (Pro), Glutamine (Gln), Glutamic acid (Glu), Leucine (Leu), Glycine (Gly), Tryptophan (Trp), Tyrosine (Tyr), Histidine (His), Phenylalanine (Phe)), anions ( $\text{S}^{2-}$ ,  $\text{HS}^-$ ,  $\text{SCN}^-$ ,  $\text{HSO}_3^-$ ,  $\text{SO}_3^{2-}$ ,  $\text{SO}_4^{2-}$ ,  $\text{CO}_3^{2-}$ ,  $\text{HCO}_3^-$ ,  $\text{NO}_3^-$ ,  $\text{NO}_2^-$ ,  $\text{AcO}^-$ ,  $\text{ClO}^-$ ,  $\text{I}^-$ ,  $\text{Br}^-$ ,  $\text{Cl}^-$  and  $\text{F}^-$ ) and cations ( $\text{Na}^+$ ,  $\text{K}^+$ ,  $\text{Mg}^{2+}$ ,  $\text{Ca}^{2+}$ ,  $\text{Ba}^{2+}$ ,  $\text{Al}^{3+}$ ,  $\text{Pb}^{2+}$ ,  $\text{NH}_4^+$ ,  $\text{Cr}^{3+}$ ,  $\text{Mn}^{2+}$ ,  $\text{Fe}^{2+}$ ,  $\text{Fe}^{3+}$ ,  $\text{Co}^{2+}$ ,  $\text{Ni}^{2+}$ ,  $\text{Cu}^{2+}$ ,  $\text{Zn}^{2+}$ ,  $\text{Cd}^{2+}$  and  $\text{Hg}^{2+}$ .) were prepared with distilled water.

### Optical Responses.

For typical absorption and fluorescence spectra measurements, **MICA** was diluted to  $5 \mu\text{M}$  in PBS buffer (10 mM, pH 7.4, with 15% DMF, V/V). 3.0 mL of the resulting solution was placed in a 10

mm path length quartz cell. Then the UV-vis or fluorescence spectra were recorded before and after (about 10 min) the addition of 10 equiv. analytes with stirring at 37 °C. The fluorescence spectra collection conditions were optimized as the excitation wavelength  $\lambda_{\text{ex}} = 400$  nm, slit width:  $d_{\text{ex}} = d_{\text{em}} = 5$  nm.

### **Kinetic Measurements.**

The 3 mL solution of **MICA** (final concentration was 5  $\mu\text{M}$  in PBS buffer (10 mM, pH 7.4, with 15% DMF, V/V) was kept in a 10 mm path length quartz cell. After the addition of Cys (1, 2, 5, 10 and 50 equiv. in PBS buffer (10 mM, pH = 7.4) to start the reaction. The time trace of the reaction was followed by monitoring 464 nm fluorescence intensity changes for the released **HMIC** during the reaction of **MICA** with Cys. ( $\lambda_{\text{ex}} = 400$  nm, slit width:  $d_{\text{ex}} = d_{\text{em}} = 0.7$  nm).

The reaction of the **MICA** with Cys was performed in a 10 mm path length UV-vis quartz cell, which was held in a Unisoku thermostated cell holder USP-203 ( $37 \pm 0.5$  °C) with stirring. After the 3 mL solution of **MICA** (final concentration was 50  $\mu\text{M}$  in DMF-PBS buffer (1:1, V/V, 10 mM, pH 7.4)) was kept at  $37 \pm 0.5$  °C for several minutes. Then the Cys solution (1, 2, 5, 10 and 50 equiv.) in PBS buffer (10 mM, pH = 7.4) was added to the above solution to start the reaction. The spectral changes and the time courses of the reactions were monitored by following the absorbance changes at 379 nm for **MICA** and 397 nm for the released **HMIC** during the reaction of **MICA** with Cys.

### **Optical Titrations of Probe by Cys.**

For typical absorption and fluorescence titration, 2.0 mL **MICA** (5  $\mu\text{M}$  PBS buffer (10 mM, pH 7.4, with 15% DMF, V/V) at 37 °C solutions was kept in a 10 mm path length quartz UV-vis or FL cell and deaerated by  $\text{N}_2$  gas for 10 min then sealed. 0.2–50 equiv. Cys (in PBS buffer, 10 mM, pH = 7.4) was added to the cell every time. After stirring 10 min at 37 °C, the absorption (at 37 °C) and fluorescence (at rt) spectra were recorded every time. The final Cys concentrations were within 0–50 equiv. vs. the probe. The detection limit (DL) was calculated with the following equation:  $\text{DL} = 3\sigma/k$ . Where  $\sigma$  is the standard deviation of the ratio fluorescence intensity 464 nm (for fluorescence spectra) or 397 nm absorbance (for absorption spectra) of the **MICA** (5  $\mu\text{M}$  PBS buffer (10 mM, pH 7.4, with 15% DMF, V/V)) in 30 times separate measurements, and  $k$  is the slope of the linear response (plot of  $I_{464 \text{ nm}}$  or  $A_{397 \text{ nm}}$  vs. Cys concentration).

### **Cell Culture and Cytotoxicity Assay.**

Cytotoxicity was investigated by the MTT [3-(4,5-dimethyl-2-thiazolyl)-2,5-diphenyl-2H-tetrazolium bromide] method. HeLa cells were seeded in a 96-well culture plate with a Dulbecco's Modified Eagle's Medium (DMEM, 10% FBS (fetal bovine serum), 100 mg/mL penicillin and

100 g/mL streptomycin) and cultured in a 5% CO<sub>2</sub>, humidified incubator for 24 h at 37 °C. The cells were treated in quintuplicate wells with each concentration of neat test compounds (final concentration of 1, 5, 10 and 15 μM in DMEM (DMF < 0.4%, including a vehicle control)) then incubated for 24 h in the dark. After removing the medium, the cells were washed 3 times with isotonic saline solution then incubated with MTT (0.5 mg/mL in isotonic saline solution, 100 μL each well) for 4 h. After removing the medium, 200 μL DMSO was added to each well to dissolve the formazan crystals. Then the 490 nm and 750 nm (reference wavelength) absorbance were measured by a microplate reader.

The cell viability was calculated as follows:

Cell viability (%) = (average absorbance of treatment group - average absorbance of the blank group) / (average absorbance of the control group - average absorbance of the blank group)

### **Cell Fluorescence Imaging.**

HeLa cells were seeded in the petri dish with a DMEM medium and cultured in a 5% CO<sub>2</sub>, humidified incubator for 24 h at 37 °C and allowed to adhere to the petri dish. Before the analyte treatment or the fluorescence imaging, the cells were washed with isotonic saline solution 3 times.

**Imaging of the endogenous Cys in HeLa cells:** The cells were incubated with **MICA** (10 μM in isotonic saline solution, 0.2% DMF) for 30 min at 37 °C. After the cells were rinsed with isotonic saline solution 3 times, then the endogenous Cys in the cells were immediately imaged by confocal fluorescence microscope ( $\lambda_{\text{ex}} = 405 \text{ nm}$ ,  $\lambda_{\text{em}} = 430\text{--}480 \text{ nm}$ ).

**Imaging of the exogenous Cys in HeLa cells:** To inhibit the endogenous Cys in the cells, two groups of HeLa cells were incubated with NEM (*N*-ethylmaleimide, 1 mM in isotonic saline solution) for 2 times, 20 min per time at 37 °C. After the cells were washed with isotonic saline solution to remove residual NEM, one group of HeLa cells were incubated with **MICA** (10 μM, 30 min) at 37 °C, then washed and imaged immediately. Before the treatment with **MICA**, another group of HeLa cells was pre-incubated with Cys (200 μM in isotonic saline solution, 1 h) at 37 °C.

**Imaging of the CO photo-releasing in HeLa cells:** To track the CO photo-releasing process of the activated **HMIC** (by the sensing reaction of the probe with Cys in HeLa cells), the **MICA** pre-treated HeLa cells were imaged by confocal fluorescence microscope. Then the HeLa cells were imaged (1 s interval time) in the green channels ( $\lambda_{\text{ex}} = 405 \text{ nm}$ ,  $\lambda_{\text{em}} = 430\text{--}480 \text{ nm}$ ) with continuous irradiation by 405 nm laser (0.83 mW with 14.8% laser power) under air at rt.

### **Zebrafish Fluorescence Imaging.**

**Imaging of the endogenous Cys in zebrafish:** The eggs of zebrafish were hatched in an E3 embryo medium at 29 °C and cultured. The 3-day-old zebrafish were imaged as a control and the

imaging conditions are optimized as  $\lambda_{\text{ex}}$ : 375-425 nm and green channel:  $\lambda_{\text{em}}$ : 460–560 nm. Four groups of the 3-days-old zebrafish were incubated with **MICA** (10  $\mu\text{M}$  in E3 embryo medium (0.2% DMF)) at 29 °C respectively for 10, 20, 30, 40 and 50 min, then washed with culture medium and imaged respectively.

**Imaging of the exogenous Cys in zebrafish:** To inhibit the endogenous Cys in zebrafish, three groups of 5-day-old zebrafish were incubated with NEM (0.1 mM in E3 embryo medium, 15 min) at 29 °C. After the zebrafish were washed with isotonic saline solution to remove residual NEM, one group of zebrafish was incubated with **MICA** (10  $\mu\text{M}$ , 30 min) at 29 °C, then washed and imaged immediately. The imaging conditions are optimized as  $\lambda_{\text{ex}}$ : 375-425 nm, green channel:  $\lambda_{\text{em}}$ : 460–560 nm. Before the treatment with **MICA**, the other three groups of zebrafish were respectively pre-incubated with 50, 100 and 200  $\mu\text{M}$  Cys (in E3 embryo medium, 30 min) at 29 °C.

### **CO Photo-Releasing Reaction Kinetics and Their Products Analysis.**

**CO Photo-Releasing Reaction Kinetics:** The O<sub>2</sub> saturated solution of **HMIC** (10  $\mu\text{M}$  in 3 mL DMF-PBS buffer (1:1, V/V, 10 mM, pH 7.4) was irradiated by visible light (intensity =  $8.25 \times 10^3$  lx) with stirring at rt. The absorption and fluorescence spectra were recorded respectively in 2–5 min time interval until the reaction was finished. The reaction process was monitored by the disappearance of the 397 nm absorbance or the 464 nm fluorescence intensity (accompanying the bright cyan fluorescence quenching).

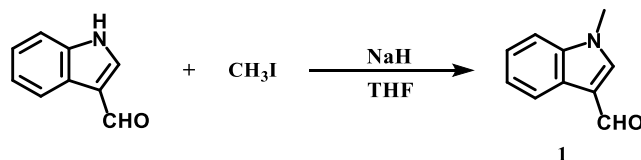
**Gas Product Analysis:** In a fixed volume flask, the O<sub>2</sub> saturated solution of **HMIC** (the desired concentration (10–50  $\mu\text{M}$ ) in 1 mL ethanol) was irradiated by visible light (intensity =  $4.75 \times 10^3$  lx) for the desired time with stirring at rt. The photoreaction process was followed by monitoring the disappearance of the bright cyan fluorescence using a 365 nm UV lamp. The irradiation was stopped until the **HMIC** was completely decomposed. After the visible light irradiation, the reaction solution was stirred for 12 minutes. Then the headspace gas (1 mL), including released CO, was injected into a Gas Chromatography with an FID (flame ionization detector) (CO was reduced to methane by translation stove) (5A column (TDX-01: 4 mm  $\times$  3 m, Column number: TL0686)). The GC spectra were recorded and the concentration and yield of the released CO were calculated using the standard calibration curve.

**Organic Product Analysis:** After the reaction in DMF, the reaction solution was dissolved in 5 mL of ethanol (total 0.1 mM). The reaction mixture was injected into HPLC-MS for organic products analysis with an online DAD detector ( $\lambda$ : 254 nm) at rt. The analysis conditions are as follows. Column: Hypersil GOLD C18 column, Thermo Fisher Scientific 150 mm  $\times$  2.1 mm, 5

$\mu\text{M}$ ; Mobile phase: MeOH and HOAc-NH<sub>4</sub>OAc buffer solution (5 mM, pH = 3) with some gradient;  
Flow rate: 0.5 mL min<sup>-1</sup>.

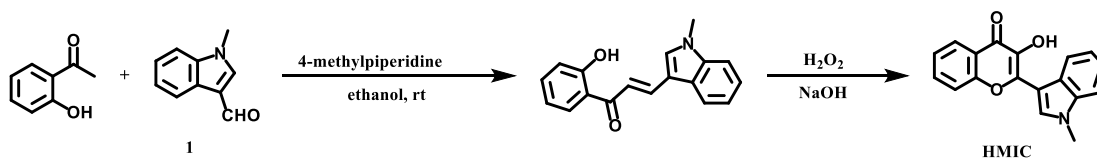
### Synthesis of the probe MICA

(a) **1** (1-methyl-1*H*-indole-3-carbaldehyde) was synthesized (yield: 97%) according to the following procedure (Scheme S1).<sup>1</sup>



**Scheme S1.** The synthesis procedure of **1**.

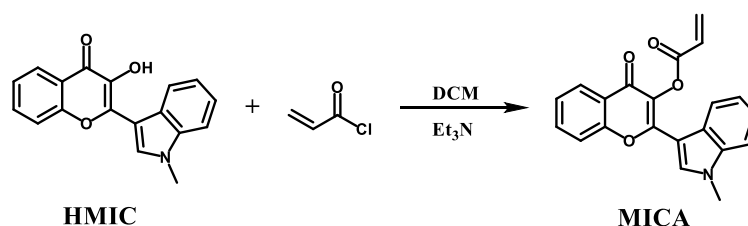
(b) **HMIC** was synthesized (yield: 83%) according to the following procedure (Scheme S2)<sup>2</sup> and characterized by <sup>1</sup>H NMR and <sup>13</sup>C NMR (FigureS20, Figure S21).



**Scheme S2.** The synthesis procedure of **HMIC**.

In a 100 mL flask, compound **1** (1.59 g, 10 mmol) was dissolved in 50 mL absolute ethanol, after stirring at 75 °C for 30 min, 2'-Hydroxyacetophenone (1.20 mL, 10 mmol) was added into the flask. The reaction solution was refluxed at 75°C with stirring for 12 h, and yellow crystals gradually precipitated in the solution. After cooled to room temperature, the reaction solution was filtered and obtained yellow crystals. The obtained yellow crystals were dissolved in methanol, and NaOH (4 g, 100 mmol) was added into solution. After stirring for 30 min, 5 mL hydrogen peroxide (30%, 45 mmol) was slowly added dropwise with stirring at room temperature. After the reaction was completed, 50 mL ice water was added, followed by adjust the pH to neutrality. The solution was filtered to obtain the yellow solids. The obtained yellow solids were purified by recrystallization from CH<sub>2</sub>Cl<sub>2</sub> to obtain 2.4 g yellow microcrystals in 83% yield. <sup>1</sup>H NMR [(CD<sub>3</sub>)<sub>2</sub>SO, 500 MHz]:  $\delta$  (ppm) = 9.50 (s, 1H), 8.46 (d,  $J$  = 8.0 Hz, 1H), 8.37 (s, 1H), 8.13 (dd,  $J$  = 7.9, 1.4 Hz, 1H), 7.92 (d,  $J$  = 8.4 Hz, 1H), 7.81–7.76 (m, 1H), 7.61 (d,  $J$  = 7.9 Hz, 1H), 7.48 (t,  $J$  = 7.5 Hz, 1H), 7.37–7.29 (m, 2H), 3.95 (s, 3H); <sup>13</sup>C NMR [(CD<sub>3</sub>)<sub>2</sub>SO, 500 MHz]:  $\delta$  (ppm) = 170.93, 154.46, 148.28, 137.16, 136.47, 134.57, 133.15, 125.47, 125.10, 124.87, 123.12, 122.46, 122.39, 121.77, 118.51, 111.12, 105.81, 33.65 (18 signals expected and observed).

(c) **MICA** was synthesized (yield: 92%) according to the following procedure (Scheme S3) and characterized by FT-IR,  $^1\text{H}$  NMR,  $^{13}\text{C}$  NMR and HRMS (FigureS16–Figure S19).



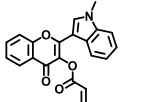
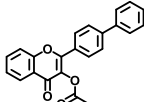
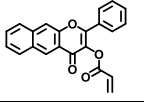
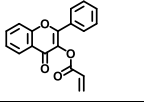
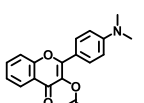
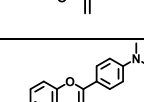
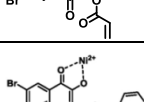
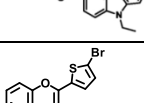
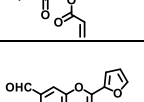
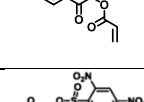
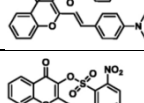
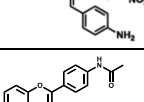
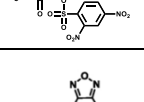
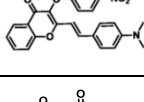
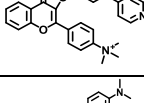
**Scheme S3.** The synthesis procedure of **MICA**.

The mixture of **HMIC** (0.29 g, 1 mmol) and triethylamine (1 mL, 7.2 mmol) was stirred at  $-5\text{ }^\circ\text{C}$  for 30min, then acryloyl chloride (0.16 mL, 1.5 mmol) was slowly added into the mixture. The reaction mixture was stirred at  $-5\text{ }^\circ\text{C}$  for 8 h. After the completion of the reaction, **MICA** was extracted with dichloromethane, and then the organic phase was washed with water, dried over anhydrous  $\text{Na}_2\text{SO}_4$ , filtered, and the filtrate was concentrated under reduced pressure. The obtained crude product (gray-white solid) was purified by column chromatography ( $R_f = 0.46$ , petroleum ether/ethyl acetate = 1:1). Subsequently, it was further purified by recrystallization from petroleum ether/ethyl acetate (5:1) to obtain white solid pure product (0.32 g, 92%). HRMS (ESI):  $m/z$  (pos.):  $[\text{M} + \text{H}]^+$ : 346.1077,  $[\text{M} + \text{Na}]^+$ : 368.0900.  $^1\text{H}$  NMR ( $\text{CDCl}_3$ , 400 MHz):  $\delta$  (ppm) = 8.36 (dd, 1 H,  $J = 6.3, 2.2$ ), 8.30 (dd, 1 H,  $J = 7.9, 0.8$ ), 7.79 (s, 1 H), 7.75–7.64 (m, 2 H), 7.47–7.33 (m, 4 H), 6.77 (d, 1 H,  $J = 17.2$ ), 6.53 (dd, 1 H,  $J = 17.3, 10.5$ ), 6.15 (d, 1 H,  $J = 10.6$ ), 3.88 (s, 3 H);  $^{13}\text{C}$  NMR ( $\text{CDCl}_3$ , 500 MHz):  $\delta$  (ppm) = 169.68, 161.72, 154.77, 154.14, 135.91, 132.56, 132.16, 132.00, 126.32, 124.92, 124.80, 123.82, 122.75, 122.30, 121.13, 120.97, 116.62, 108.98, 104.11, 32.64 (21 signals expected and observed).

## Reference

1. Chen, K.; Zhang, Y. L.; Fan, J.; Ma, X.; Qin, Y. J.; Zhu, H. L. Novel Nicotinoyl Pyrazoline Derivates Bearing N-Methyl Indole Moiety as Antitumor Agents: Design, Synthesis, and Evaluation. *Eur. J. Med. Chem.* **2018**, *156*, 722–737.
2. Venturella, P.; Bellino, A.; Piozzi, F. Synthesis of indolylchalcones and indolylchromonols. *Farmaco, Edizione Scientifica.* **1971**, *26*(7), 591–6.

**Table S1.** Comparison of the flavonol-based fluorescent probes and photoCORMs.

compounds	analyte	<i>c</i> (probe) ( $\mu\text{M}$ )	medium	ratio	Quantum yield $\Phi$	response time	detection limit	linear range (equiv.)	Reference
	Cys	5	PBS buffer (10 mM, pH 7.4, with 15% DMF, V/V)	I <sub>464</sub>	0.471	330 s	92 nM	0–2.4	This work
	Cys	5	DMSO:PBS (1:1 V/V, 10 mM, pH = 7.4)	I <sub>546</sub> / I <sub>443</sub>	0.069	45 s	18.5 nM	0–1	<i>J. Mater. Chem. B</i> <b>2021</b> , <i>9</i> , 8263–8271.
	Cys	10	CH <sub>3</sub> CN:PBS (1:1 V/V, w/3% DMSO, 10 mM, pH = 7.4)	I <sub>490</sub>		~3 min	24 nM	0.17–1	<i>J. Am. Chem. Soc.</i> <b>2017</b> , <i>139</i> , 9435–9438.
	Cys	10	MeCN:H <sub>2</sub> O (1:1, V/V) solution with 10 mM HEPES buffer.	I <sub>510</sub>	0.53	60 min	< 1 $\mu\text{M}$	1–10	<i>ACS Appl. Mater. Interfaces</i> <b>2014</b> , <i>6</i> , 4402–4407.
	Cys	20	20 mM PBS buffer (pH 7.4) with 20% DMSO (V/V)	I <sub>550</sub>	0.025	~5 min	~0.2 $\mu\text{M}$	0–1	<i>ACS Appl. Mater. Interfaces</i> <b>2014</b> , <i>6</i> , 17543–17550.
	Cys	10	DMSO:PBS (1:1, V/V, pH = 7.4)	I <sub>568</sub>	0.47	5 min	1.87 nM	1–8	<i>Talanta</i> <b>2018</b> , <i>181</i> , 118–124.
	Cys Hcy	10	1-Ni <sup>2+</sup> in HEPES buffer-methanol (1:9, V/V, pH = 7.4)	I <sub>527</sub>	0.47	5 min	4.06 nM 5.8 nM	1–8 1–10	<i>Talanta</i> <b>2018</b> , <i>181</i> , 118–124.
	Cys	10	DMSO:PBS (1:4 V/V, 10 mM, pH = 7.4)	I <sub>530</sub> / I <sub>420</sub>	0.158	~15 min	42.3 nM	0–3	<i>Talanta</i> <b>2019</b> , <i>194</i> , 717–722.
	Cys	20	CH <sub>3</sub> CN:PBS (4:6 V/V, 10 mM, pH = 7.4)	I <sub>525</sub>		10 min	37.9 nM	0–20	<i>Chinese Journal of Analytical Chemistry</i> , <b>2020</b> , <i>48</i> , 1033–1040.
	Cys Hcy GSH	10	HEPES buffer with 30% acetonitrile	I <sub>632</sub>	0.15	>15 min >60 min >60 min	0.07 $\mu\text{M}$ 0.18 $\mu\text{M}$ 0.12 $\mu\text{M}$	0–0.6 0–0.6 0–0.6	<i>RSC Adv.</i> <b>2013</b> , <i>3</i> , 11543–11546.
	GSH	20	50 mM Tris-buffer (pH 7.4)	I <sub>497</sub>		~60 min	0.90 $\mu\text{M}$	0–0.5	<i>Sensors Actuators, B Chem.</i> <b>2018</b> , <i>262</i> , 144–152.
	GSH	20	50 mM Tris-buffer (pH 7.4)	I <sub>543</sub>		~60 min	0.97 $\mu\text{M}$	0–0.5	<i>Sensors Actuators, B Chem.</i> <b>2018</b> , <i>262</i> , 144–152.
	Cys Hcy GSH	5	PBS buffer (10.0 mM, pH 7.4, containing 30% CH <sub>3</sub> CN, V/V).	I <sub>545</sub> I <sub>621</sub>		~60 min ~120 min ~70 min	2.1 $\mu\text{M}$ 2.7 $\mu\text{M}$ 6.4 $\mu\text{M}$	0–100 0–100 0–110	<i>Anal. Chem.</i> <b>2016</b> , <i>88</i> , 3638–3646.
	Cys	10	PBS solution (10 mM, pH = 7.4)	I <sub>520</sub>		~2 min	0.48 $\mu\text{M}$	0–2	<i>J. Photochem. Photobiol. A Chem.</i> <b>2018</b> , <i>355</i> , 72–77.
	Cys Hcy	10	DMSO:PBS buffer (7:3, V/V, 10 mM, pH 7.4).	I <sub>528</sub> I <sub>526</sub>		~30 min ~40 min	0.82 $\mu\text{M}$ 1.45 $\mu\text{M}$	2–30 1–20	<i>Talanta</i> <b>2016</b> , <i>146</i> , 41–48.

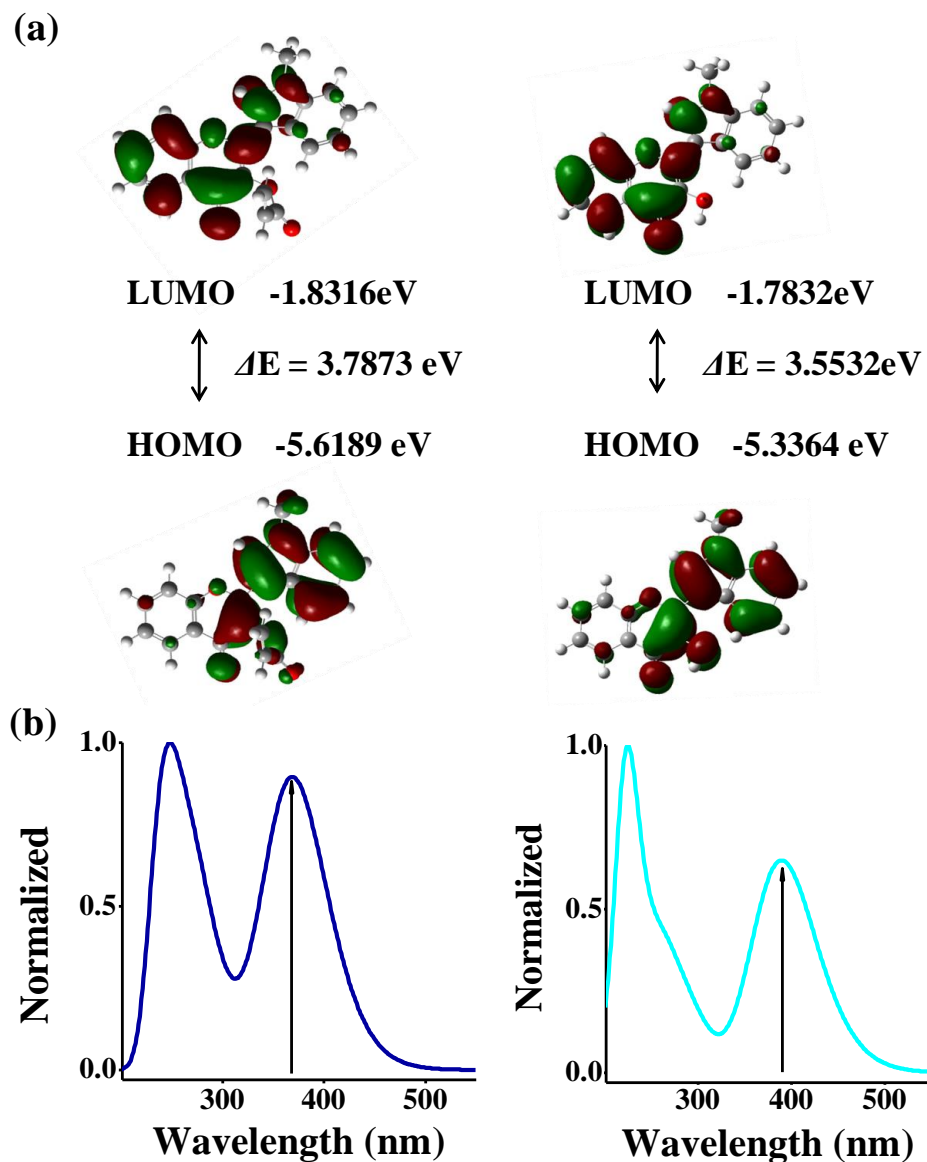


**Figure S1.** (a) Molecular orbital plots of HOMO, LUMO of the optimized structure of **MICA** and **HMIC**, and their energy levels. (b) The theoretically predicted (based on the TD-DFT calculation results) absorption spectra of **MICA** and **HMIC**.

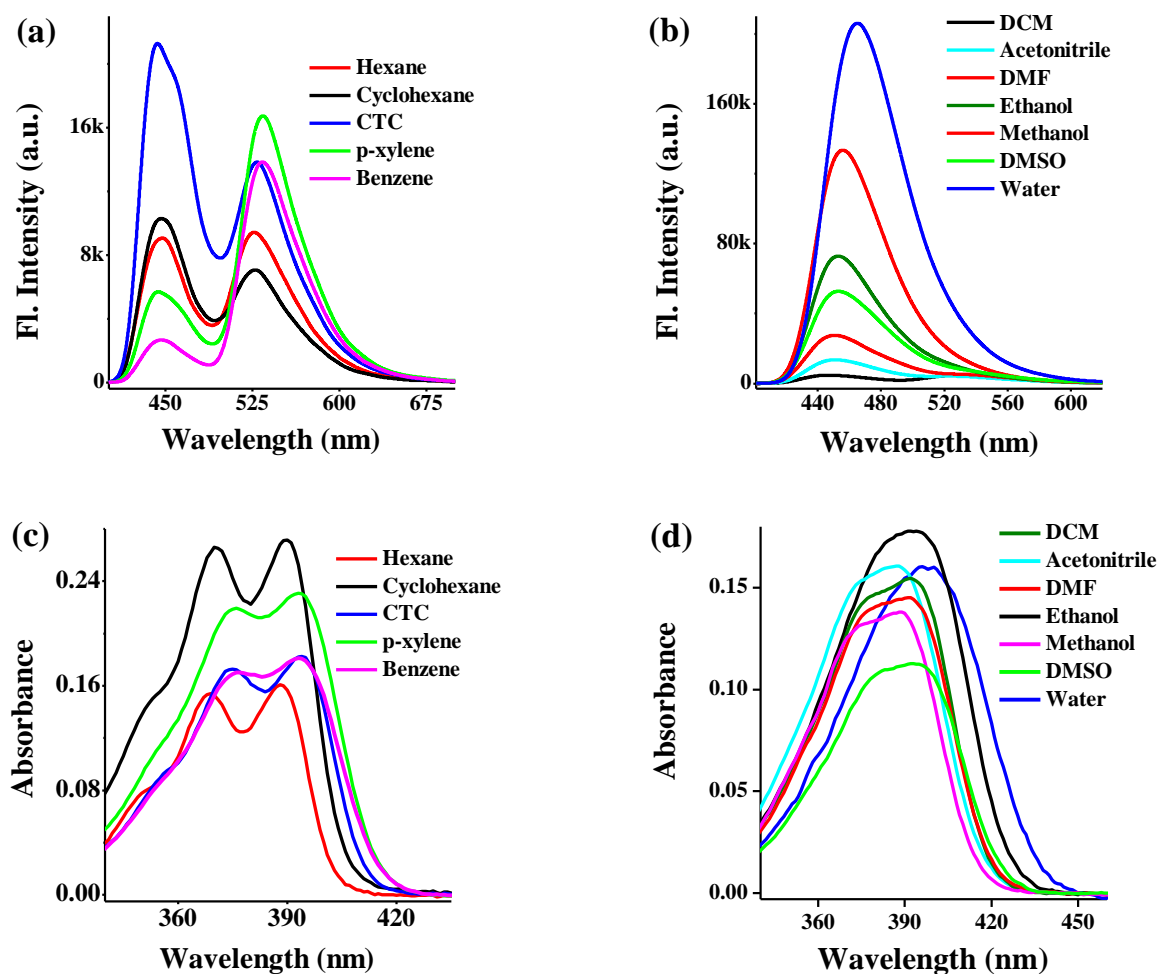


**Figure S2.** Spectral features of **HMIC** (5  $\mu\text{M}$ ) in various solvents at 37  $^{\circ}\text{C}$ . Fluorescence spectra (a) in non-polar and non-protic solvents, (b) in polar and protic solvents. ( $\lambda_{\text{ex}} = 400$  nm, slit width:  $d_{\text{ex}} = d_{\text{em}} = 5$  nm). Absorption spectra (c) in non-polar and non-protic solvents, (d) in polar and protic solvents. (In water: with 15% DMF)

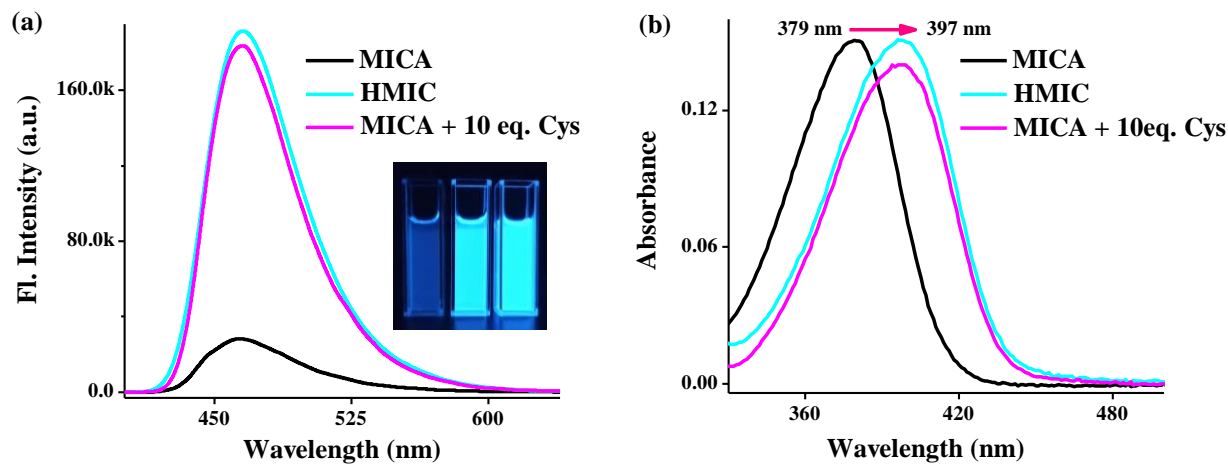


**Figure S3.** (a) Fluorescence and (b) absorption spectra of **MICA** (black), **MICA** + 10 equiv. Cys (pink) and **HMIC** (cyan). Inset: The solution color of **MICA** (left), **MICA** + 10 equiv. Cys (middle), **HMIC** (right) under 365 nm light. Conditions:  $c(\text{MICA}) = 5 \mu\text{M}$ ; PBS buffer (10 mM, pH 7.4, with 15% DMF,  $V/V$ ) at 37 °C;  $\lambda_{\text{ex}} = 400 \text{ nm}$ , slit width:  $d_{\text{ex}} = d_{\text{em}} = 5 \text{ nm}$ .

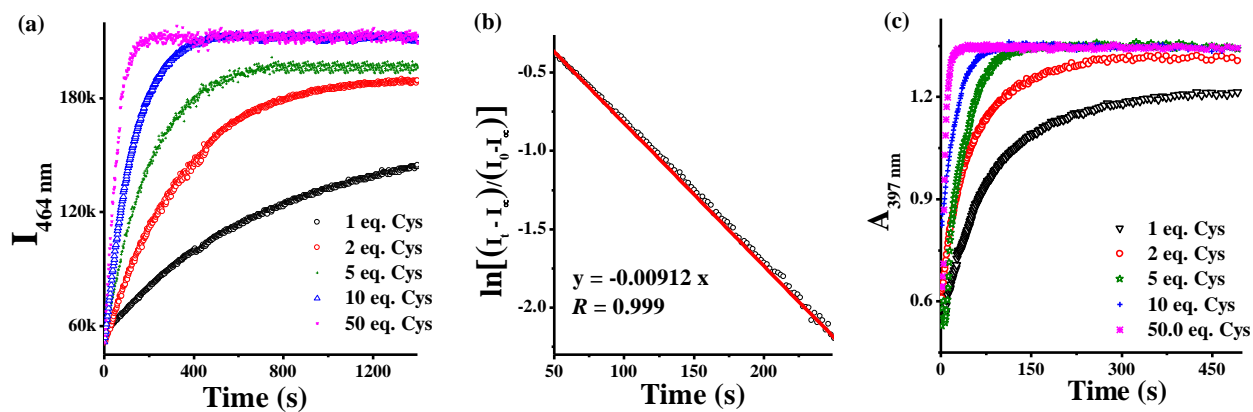


**Figure S4.** Kinetic studies of the reaction of **MICA** with varying amounts of Cys (1, 2, 5, 10 and 50 equiv.) at 37 °C. (a) Time traces of  $I_{464 \text{ nm}}$  of **MICA** (5  $\mu\text{M}$ ) with Cys in PBS buffer (10 mM, pH 7.4, with 15% DMF,  $V/V$ ). ( $\lambda_{\text{ex}} = 400 \text{ nm}$ , slit width:  $d_{\text{ex}} = d_{\text{em}} = 0.7 \text{ nm}$ ). (b) Plot of  $\ln[(I_t - I_\infty)/(I_0 - I_\infty)]$  of  $I_{464 \text{ nm}}$  vs. time (for 10 equiv. Cys). (c) Time traces of  $A_{397 \text{ nm}}$  of **MICA** (50  $\mu\text{M}$ ) with Cys in DMF-PBS buffer (1:1,  $V/V$ , 10 mM, pH 7.4).

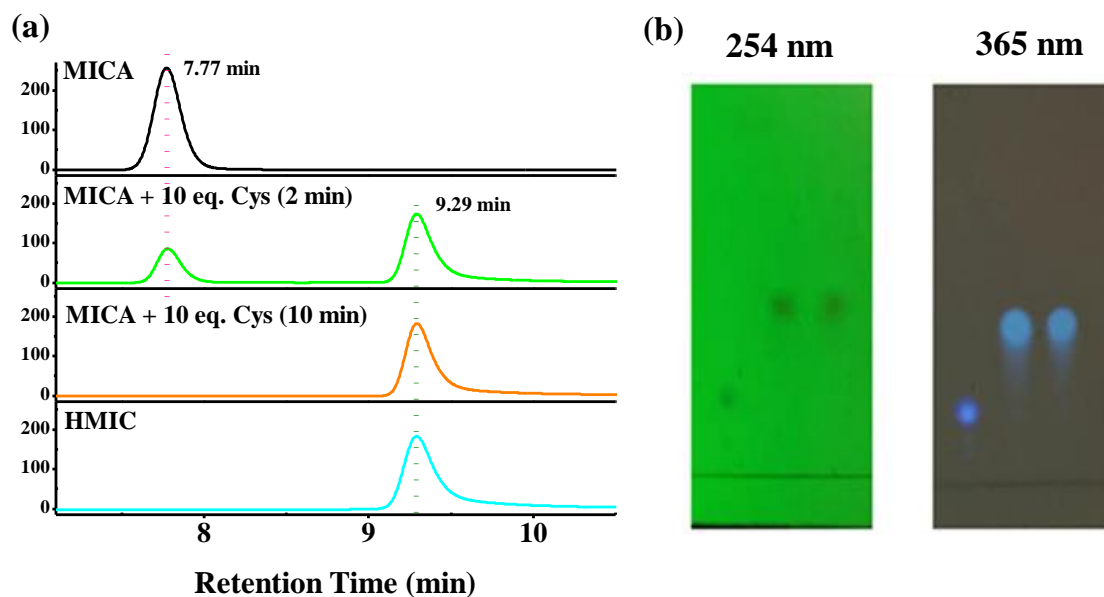


**Figure S5.** (a) HPLC spectra of **MICA** (black line), **HMIC** (cyan line), the reaction mixture of **MICA** with 10 equiv. Cys after 2 and 10 min (respectively green and orange line). (b) TLC (Mobile phase: petroleum ether: ethyl acetate = 1:1) photos of **MICA** (left), **MICA** + 10 equiv. Cys (middle), **HMIC** (right). The concentrations of all analytes are 0.1 mM in ethanol.

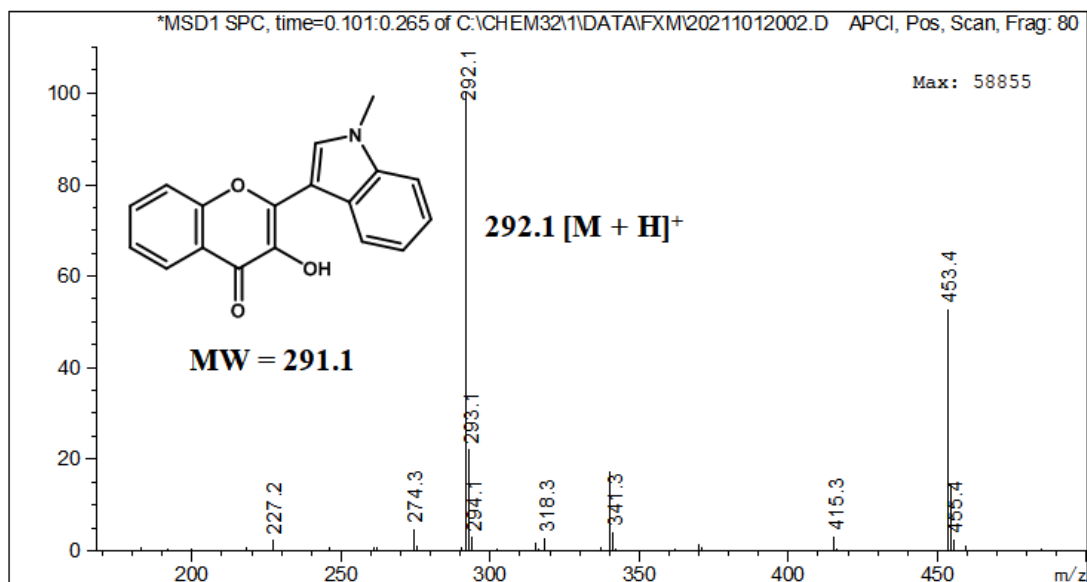


**Figure S6.** APCI-MS spectrum of the reaction solution of **MICA** (0.25 mM in ethanol) with 10 equiv. Cys (in PBS buffer, pH = 7.4).

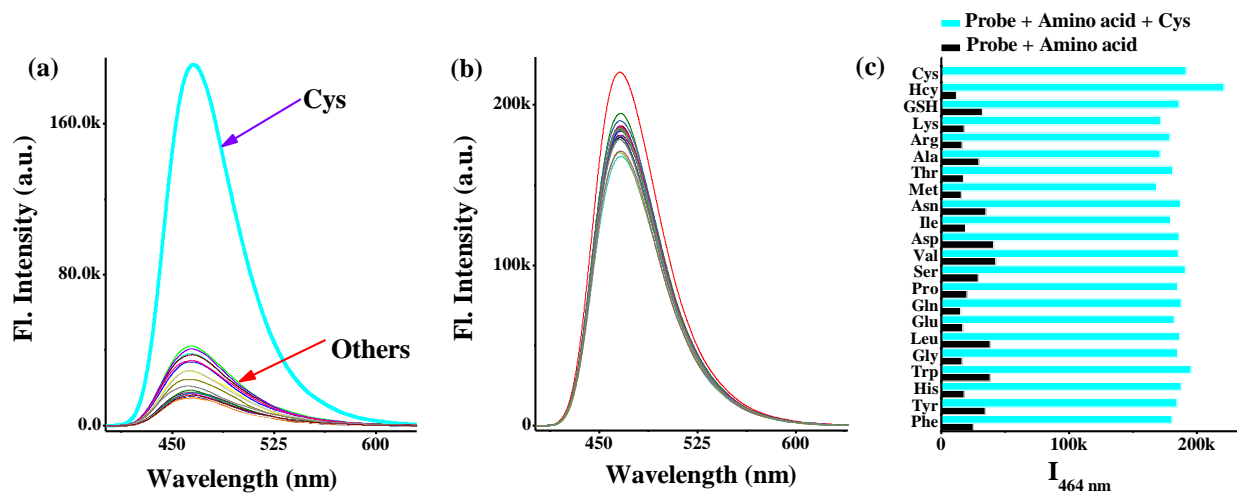


**Figure S7.** Fluorescence spectral changes of **MICA** upon addition of 10 equiv. Cys under (a) absence and (b) presence of 10 equiv. another competitive single amino acid. (c)  $I_{464 \text{ nm}}$  of **MICA** upon addition of 10 equiv. Cys under absence (black) and presence (cyan) of 10 equiv. another competitive single amino acid. Amino acids: Cys, Hcy, GSH (200 eq.), Lys, Arg, Ala, Thr, Met, Asn, Ile, Asp, Val, Ser, Pro, Gln, Glu, Leu, Gly, Trp, His, Tyr and Phe. Conditions: **MICA** = 5  $\mu\text{M}$ ; PBS buffer (10 mM, pH 7.4, with 15% DMF, V/V) at 37  $^{\circ}\text{C}$ ;  $\lambda_{\text{ex}}$  = 400 nm, slit width:  $d_{\text{ex}} = d_{\text{em}} = 5 \text{ nm}$ .

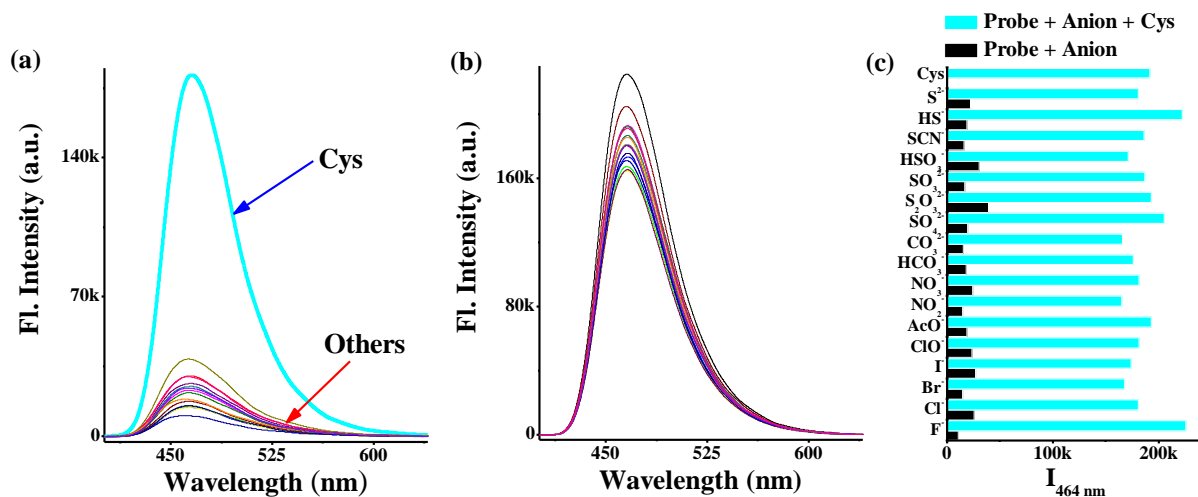


**Figure S8.** Fluorescence spectral changes of **MICA** upon addition of 10 equiv. Cys under (a) absence and (b) presence of 10 equiv. another competitive single bio-relevant anion. (c)  $I_{464 \text{ nm}}$  of **MICA** upon addition of 10 equiv. Cys under absence (black) and presence (cyan) of 10 equiv. another competitive single anion. Anions: Cys,  $S^{2-}$ ,  $HS^-$ ,  $SCN^-$ ,  $HSO_3^-$ ,  $SO_3^{2-}$ ,  $SO_4^{2-}$ ,  $CO_3^{2-}$ ,  $HCO_3^-$ ,  $NO_3^-$ ,  $NO_2^-$ ,  $AcO^-$ ,  $ClO^-$ ,  $I^-$ ,  $Br^-$ ,  $Cl^-$  and  $F^-$ . Conditions: **MICA** = 5  $\mu\text{M}$ ; PBS buffer (10 mM, pH 7.4, with 15% DMF,  $V/V$ ) at 37  $^\circ\text{C}$ ;  $\lambda_{\text{ex}}$  = 400 nm, slit width:  $d_{\text{ex}} = d_{\text{em}} = 5$  nm.

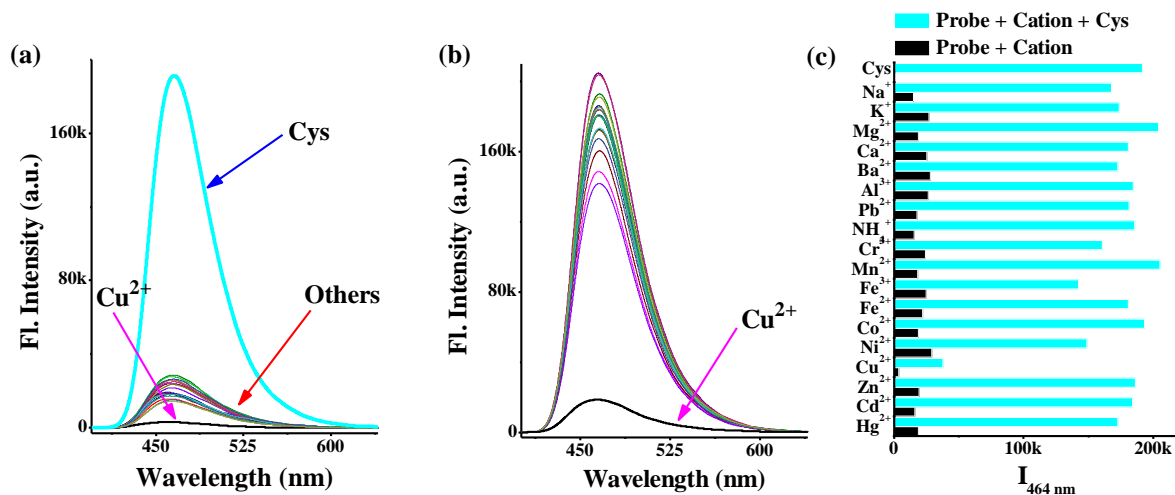


**Figure S9.** Fluorescence spectral changes of **MICA** upon addition of 10 equiv. Cys under (a) absence and (b) presence of 10 equiv. another competitive single bio-relevant cation. (c)  $I_{464 \text{ nm}}$  of **MICA** upon addition of 10 equiv. Cys under absence (black) and presence (cyan) of 10 equiv. another competitive single bio-relevant cation. Cations: Cys, Na<sup>+</sup>, K<sup>+</sup>, Mg<sup>2+</sup>, Ca<sup>2+</sup>, Ba<sup>2+</sup>, Al<sup>3+</sup>, Pb<sup>2+</sup>, NH<sub>4</sub><sup>+</sup>, Cr<sup>3+</sup>, Mn<sup>2+</sup>, Fe<sup>2+</sup>, Fe<sup>3+</sup>, Co<sup>2+</sup>, Ni<sup>2+</sup>, Cu<sup>2+</sup>, Zn<sup>2+</sup>, Cd<sup>2+</sup> and Hg<sup>2+</sup>. Conditions: **MICA** = 5  $\mu$ M; PBS buffer (10 mM, pH 7.4, with 15% DMF, V/V) at 37 °C;  $\lambda_{\text{ex}}$  = 400 nm, slit width:  $d_{\text{ex}} = d_{\text{em}} = 5$  nm.

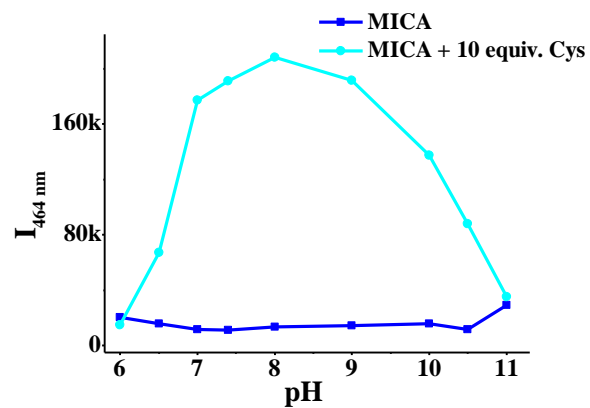


**Figure S10.** The pH dependent  $I_{464 \text{ nm}}$  of **MICA** solution ( $5 \mu\text{M}$ ) in the absence ( $\blacksquare$  blue) and presence ( $\bullet$  cyan) of 10 equiv. Cys in PBS buffer (10 mM, pH: 6–11, with 15% DMF, V/V) at  $37 \text{ }^\circ\text{C}$ . ( $\lambda_{\text{ex}} = 400 \text{ nm}$ , slit width:  $d_{\text{ex}} = d_{\text{em}} = 5 \text{ nm}$ ).

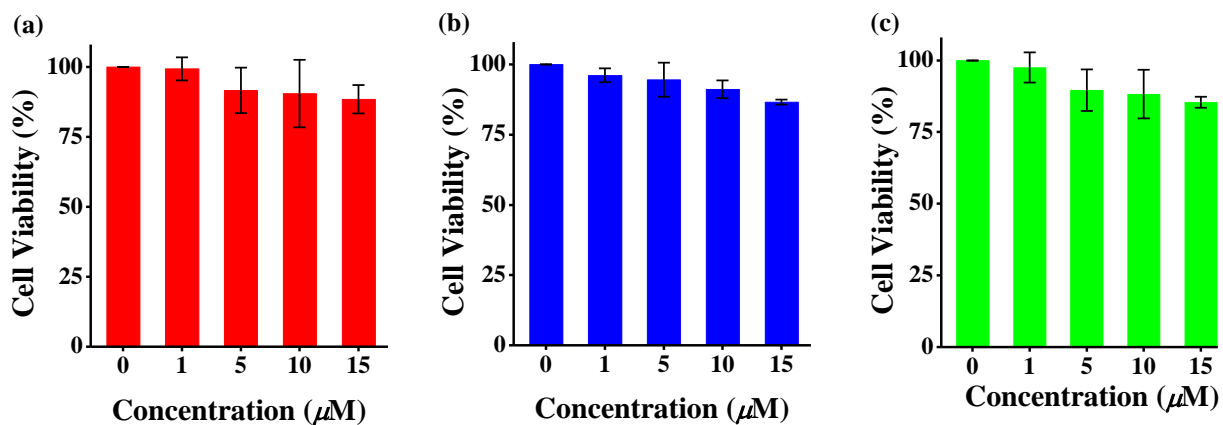


**Figure S11.** The MTT assay of HeLa cells respectively incubated with different concentrations of (a) **HMIC**, (b) **MICA** and (c) the **HMIC** photolysis products for 24 h. (0, 1, 5, 10 and 15 μM). The error bars in the column represent standard deviations of three separate measurements.

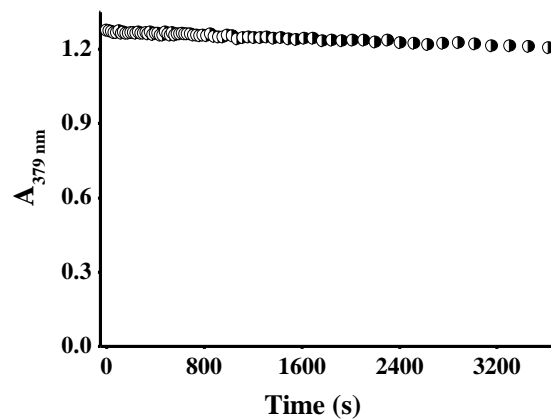


**Figure S12.** The time traces of  $A_{379\text{ nm}}$  of **MICA** ( $50\ \mu\text{M}$ ) under the presence of the esterase ( $0.1\ \text{mg}\cdot\text{L}^{-1}$  in PBS buffer,  $15\ \text{units}\cdot\text{mg}^{-1}$ ) in 3 mL DMF-PBS buffer (1:1, V/V, 10 mM, pH 7.4) at  $37\ ^\circ\text{C}$ .

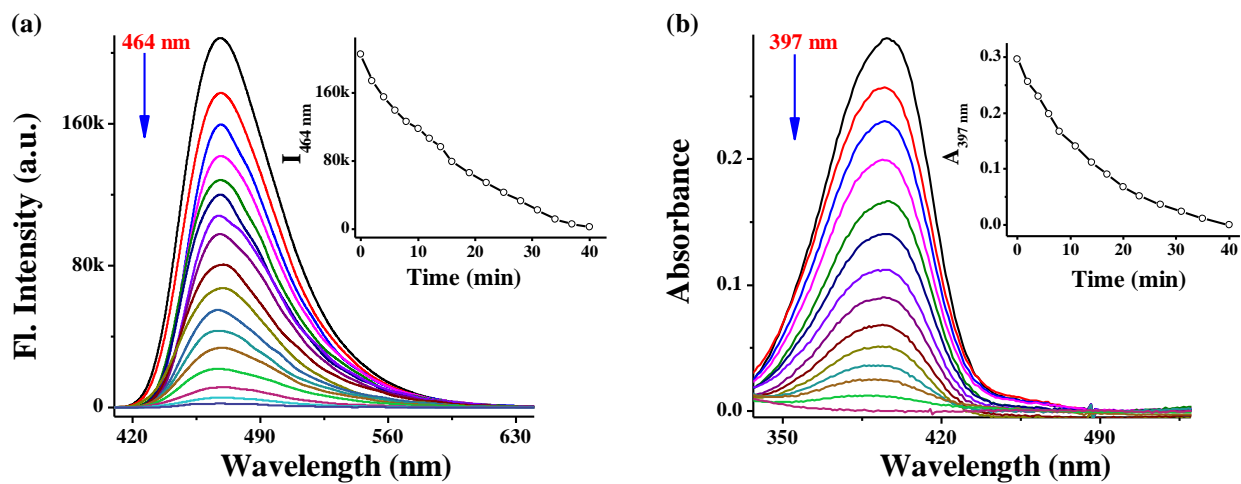


**Figure S13.** (a) Fluorescence and (b) absorption spectral changes of **HMIC** (10 μM) during visible light irradiation (intensity =  $8.25 \times 10^3$  lx) in DMF-PBS buffer (1:1, V/V, 10 mM, pH 7.4) under O<sub>2</sub> at rt. Insets: Plots of (a)  $I_{464 \text{ nm}}$  and (b)  $A_{397 \text{ nm}}$  vs. the irradiation time. Time intervals: 1 min. ( $\lambda_{\text{ex}} = 400 \text{ nm}$ , slit width:  $d_{\text{ex}} = d_{\text{em}} = 5 \text{ nm}$ ).

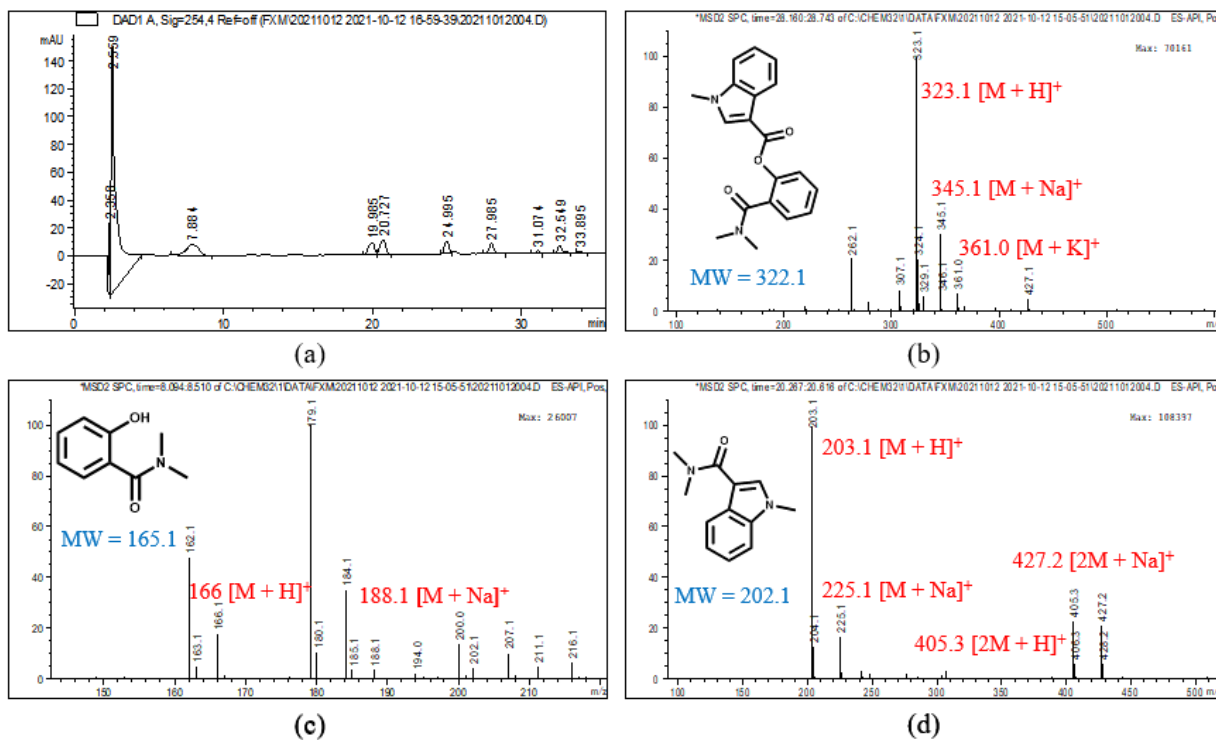


**Figure S14.** HPLC-MS spectra for the photo-reaction organic products. (a) HPLC spectrum. MS spectra of (b) 2-(dimethylcarbamoyl)phenyl 1-methyl-1*H*-indole-3-carboxylate ( $m/z$  (pos.): 323.1 ( $M + H$ )<sup>+</sup>), (c) 2-hydroxy-*N,N*-dimethylbenzamide ( $m/z$  (pos.): 166.1 ( $M + H$ )<sup>+</sup>), (d) 1-methyl-1*H*-indole-3-carboxylic acid dimethyl amid ( $m/z$  (pos.): 203.1 ( $M + H$ )<sup>+</sup>).

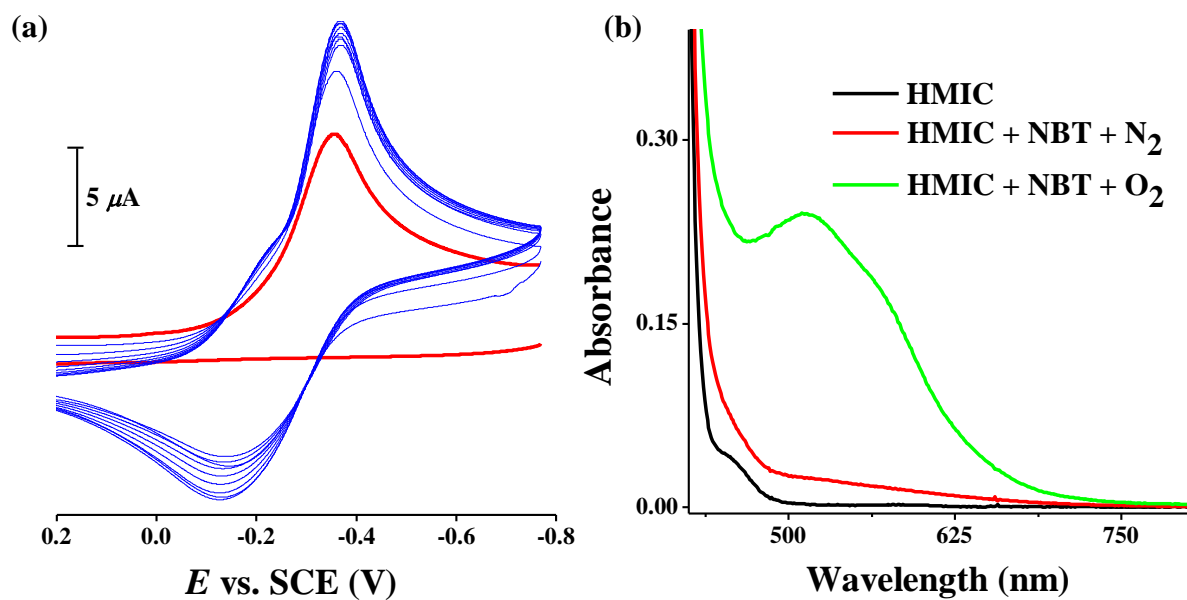


**Figure S15.** (a) Cyclic voltammograms of **HMIC** (2 mM in DMF) under N<sub>2</sub>, subsequently under air at rt. (b) Absorption spectral change of **HMIC** (0.3 mM in DMF) in the absence (under N<sub>2</sub>, black) and presence of NBT (0.45 mM) under N<sub>2</sub> (red) and O<sub>2</sub> (green) at rt.

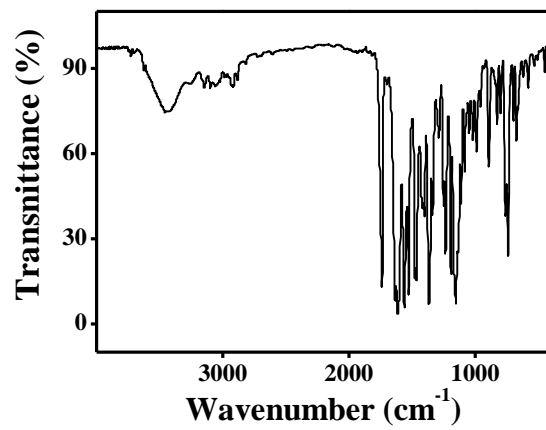


**Figure S16.** FT-IR spectra of MICA.

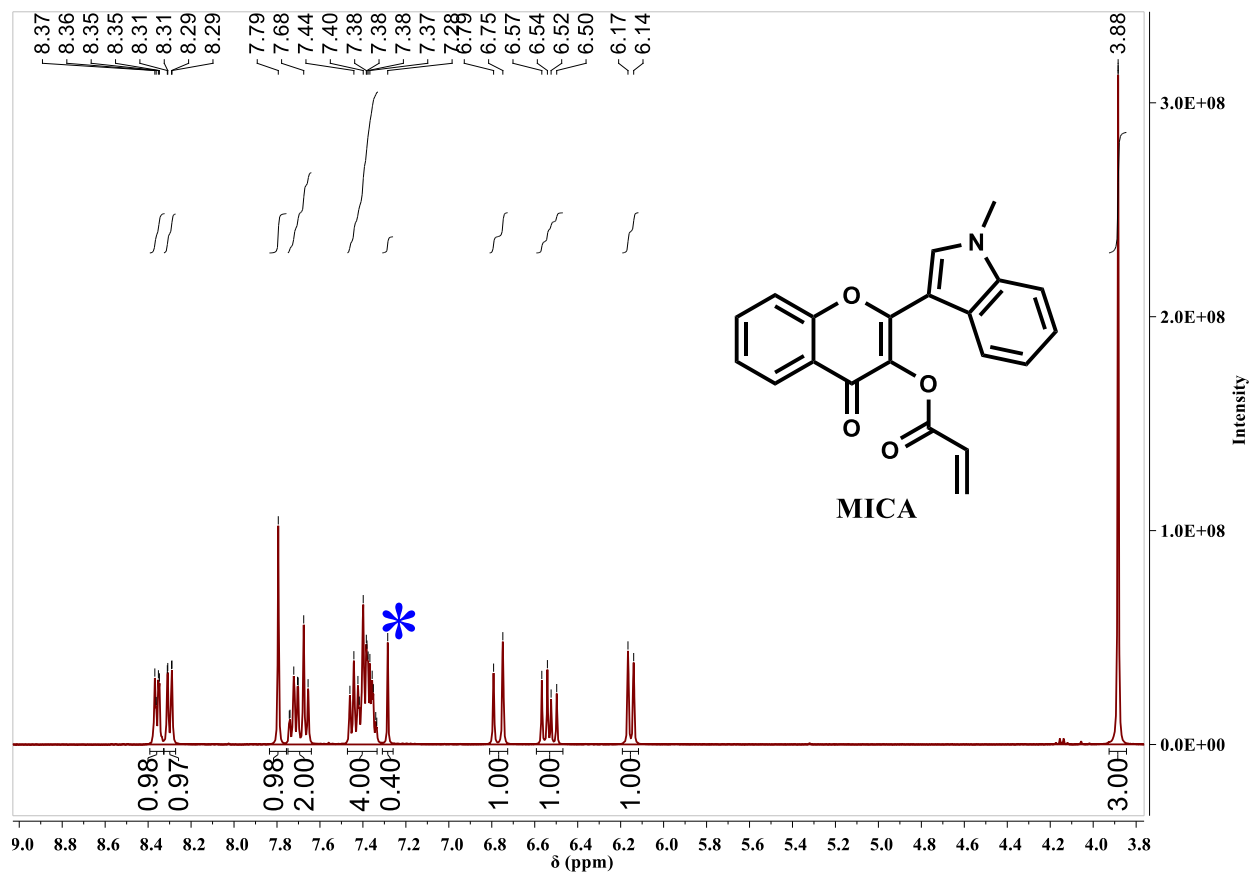


**Figure S17.**  $^1\text{H}$  NMR (400 MHz) spectrum of **MICA**. The \* indicates the signal from the residual  $\text{CDCl}_3$  in the solvent.

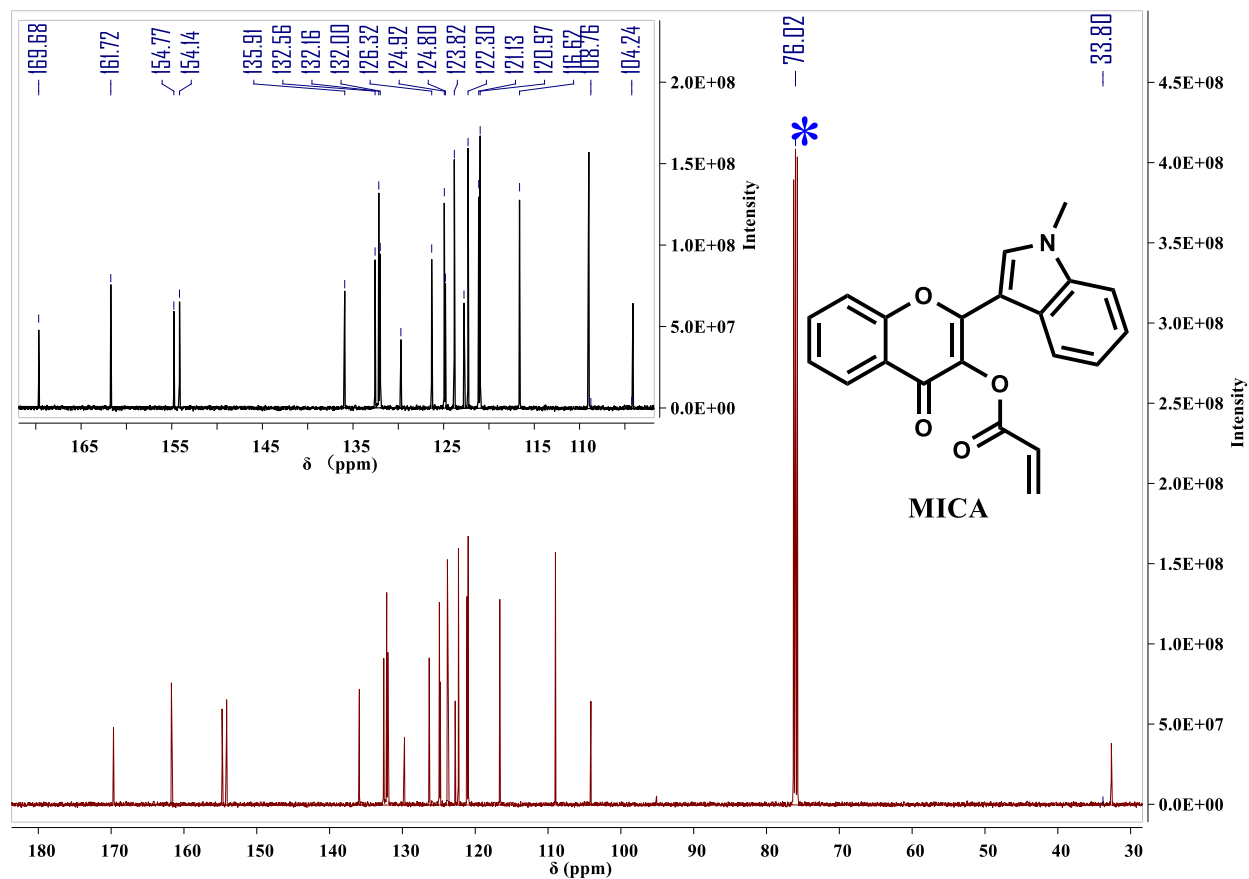


**Figure S18.**  $^{13}\text{C}$  NMR (500 MHz) spectrum of MICA. The \* indicates the signal from the  $\text{CDCl}_3$ .

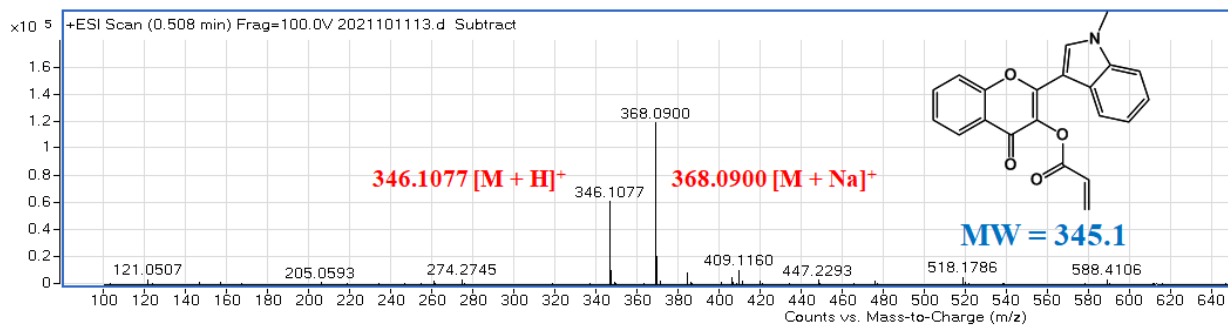


**Figure S19.** HRMS spectrum of MICA.

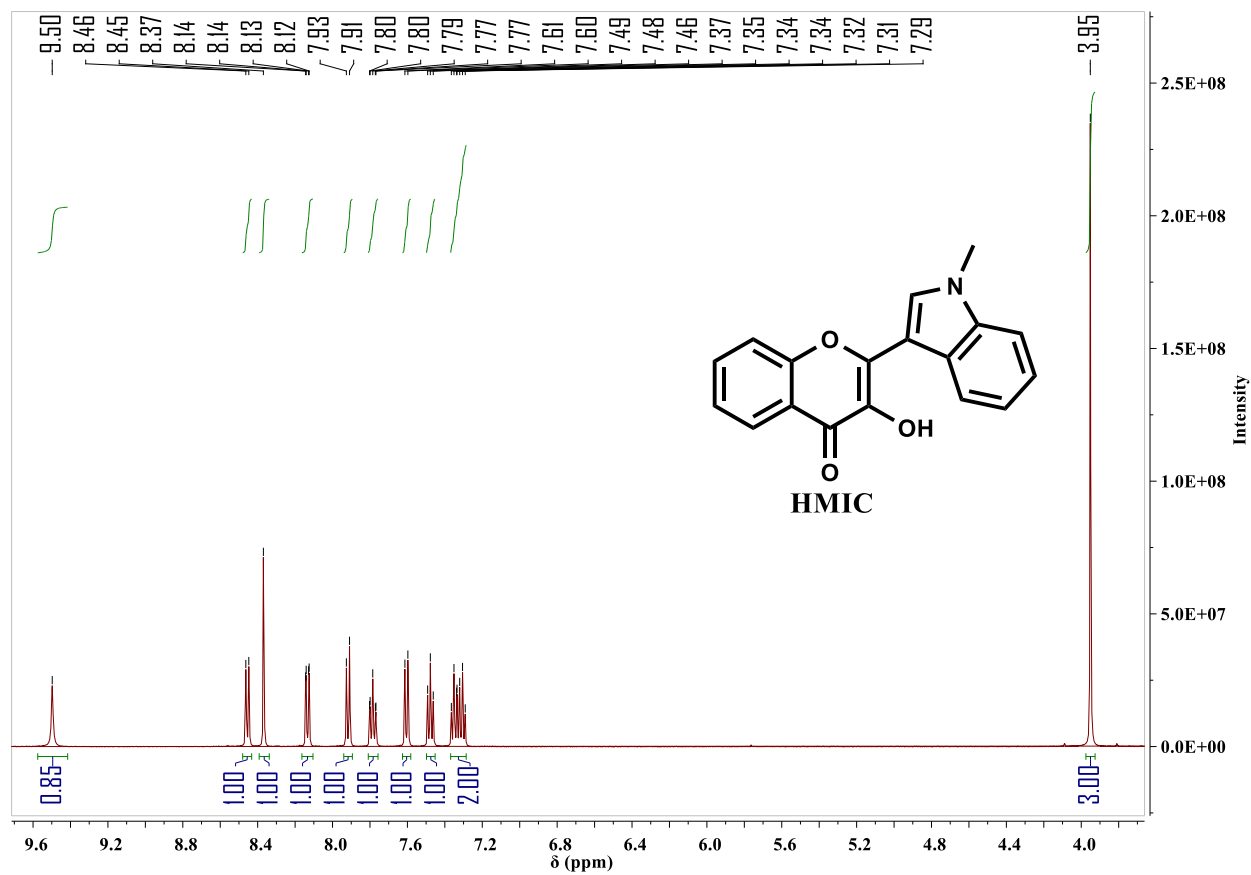


**Figure S20.**  $^1\text{H}$  NMR (500 MHz) spectrum of **HMIC** in  $(\text{CD}_3)_2\text{SO}$ .

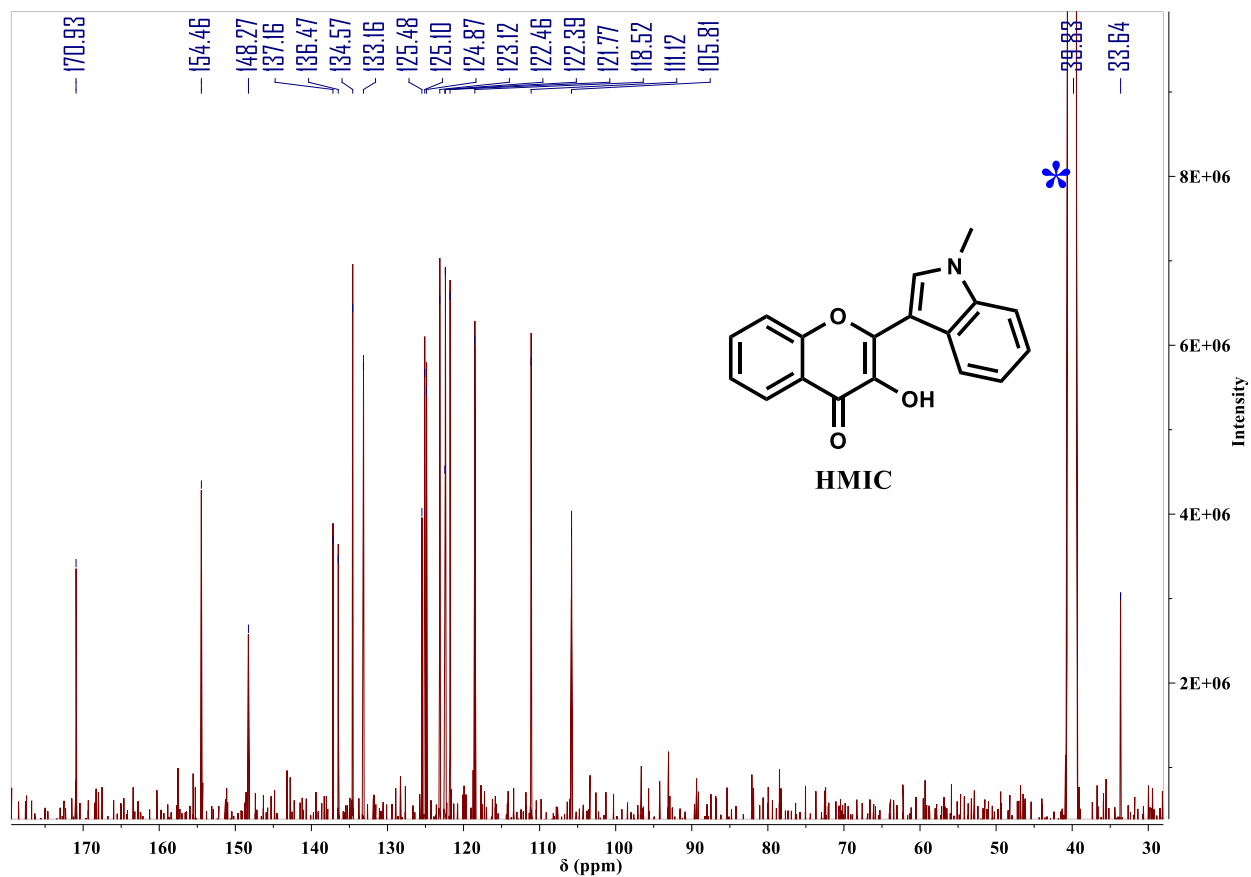


**Figure S21.**  $^{13}\text{C}$  NMR (500 MHz) spectrum of **HMIC**. The \* indicates the signal from the solvent DMSO.